Basal Levels of (p)ppGpp in *Enterococcus faecalis*: the Magic beyond the Stringent Response

Anthony O. Gaca,[a] Jessica K. Kajfasz,[a] James H. Miller,[a] Kuanqing Liu,[b] Jue D. Wang,[b] Jacqueline Abranches,[a] José A. Lemos[a]

Center for Oral Biology and Department of Microbiology and Immunology, University of Rochester Medical Center, Rochester, New York, USA[a]; Department of Bacteriology, University of Wisconsin—Madison, Madison, Wisconsin, USA[b]

ABSTRACT The stringent response (SR), mediated by the alarmone (p)ppGpp, is a conserved bacterial adaptation system controlling broad metabolic alterations necessary for survival under adverse conditions. In *Enterococcus faecalis*, production of (p)ppGpp is controlled by the bifunctional protein RSH (for "Rel SpoT homologue"; also known as RelA) and by the monofunctional synthetase RelQ. Previous characterization of *E. faecalis* strains lacking *rsh*, *relQ*, or both revealed that RSH is responsible for activation of the SR and that alterations in (p)ppGpp production negatively impact bacterial stress survival and virulence. Despite its well-characterized role as the effector of the SR, the significance of (p)ppGpp during balanced growth remains poorly understood. Microarrays of *E. faecalis* strains producing different basal amounts of (p)ppGpp identified several genes and pathways regulated by modest changes in (p)ppGpp. Notably, expression of numerous genes involved in energy generation were induced in the $\Delta rsh\ \Delta relQ$ [(p)ppGpp^0] strain, suggesting that a lack of basal (p)ppGpp places the cell in a "transcriptionally relaxed" state. Alterations in the fermentation profile and increased production of H_2O_2 in the (p)ppGpp^0 strain substantiate the observed transcriptional changes. We confirm that, similar to what is seen in *Bacillus subtilis*, (p)ppGpp directly inhibits the activity of enzymes involved in GTP biosynthesis, and complete loss of (p)ppGpp leads to dysregulation of GTP homeostasis. Finally, we show that the association of (p)ppGpp with antibiotic survival does not relate to the SR but rather relates to basal (p)ppGpp pools. Collectively, this study highlights the critical but still underappreciated role of basal (p)ppGpp pools under balanced growth conditions.

IMPORTANCE Drug-resistant bacterial infections continue to pose a significant public health threat by limiting therapeutic options available to care providers. The stringent response (SR), mediated by the accumulation of two modified guanine nucleotides collectively known as (p)ppGpp, is a highly conserved stress response that broadly remodels bacterial physiology to a survival state. Given the strong correlation of the SR with the ability of bacteria to survive antibiotic treatment and the direct association of (p)ppGpp production with bacterial infectivity, understanding how bacteria produce and utilize (p)ppGpp may reveal potential targets for the development of new antimicrobial therapies. Using the multidrug-resistant pathogen *Enterococcus faecalis* as a model, we show that small alterations to (p)ppGpp levels, well below concentrations needed to trigger the SR, severely affected bacterial metabolism and antibiotic survival. Our findings highlight the often-underappreciated contribution of basal (p)ppGpp levels to metabolic balance and stress tolerance in bacteria.

Address correspondence to José A. Lemos, jose_lemos@urmc.rochester.edu.

Despite being a commensal of the gut microbiota, the Gram-positive pathogen *Enterococcus faecalis* ranks among the leading causative agents of severe and costly nosocomial infections (1). The prevalence of *E. faecalis* in hospital settings has been attributed to its capacity to survive under adverse conditions, including prolonged starvation and exposure to detergents and commonly used antibiotics, to which *E. faecalis* has both intrinsic and acquired tolerance (2). This inherent resilience allows *E. faecalis* to survive under conditions lethal to most other bacteria, pathogenic or nonpathogenic, a trait that seems to be intertwined with its virulence.

The stringent response (SR) is a highly conserved bacterial stress response mediated by the accumulation of the alarmone (p)ppGpp, which refers to two modified guanine nucleotides, pyrophosphorylated GDP or GTP (herein abbreviated as ppGpp and pppGpp, respectively) (3). While initially defined as a response to amino acid starvation, the term SR has since expanded to include any regulatory effect exerted by robust (p)ppGpp accumulation, irrespective of the triggering mechanism. During the SR, the accumulation of (p)ppGpp induces large-scale transcriptional alterations, leading to general repression of genes required for rapid growth, such as rRNA genes, and concomitant activation of genes involved in nutrient synthesis or acquisition and stress survival, a response that shifts cellular resources toward adaptation to a non-growth state (4–7). In Gram-negative bacteria, (p)ppGpp primarily interacts with RNAP, in synergy with DksA, to directly affect

transcription (3). However, direct (p)ppGpp-RNAP interactions do not seem to occur in Gram-positive species (8, 9), and the current model suggests that (p)ppGpp affects transcription of rRNA genes in this bacterial group by reducing the availability of the initiating nucleotide GTP (8). In addition to transcriptional control, (p)ppGpp allosterically inhibits the activity of enzymes other than RNAP, including DNA primase, exopolyphosphatase, lysine decarboxylase, and several enzymes involved in GTP synthesis (10–12).

In Gram-negative proteobacteria, such as *Escherichia coli*, (p)ppGpp is metabolized by the strong (p)ppGpp synthetase RelA and the bifunctional protein SpoT, which exerts weak synthetase and strong hydrolase activities (13, 14). In Gram-positive organisms, the bifunctional protein RSH (for "Rel SpoT homologue"), also known as RelA or Rel, is a strong (p)ppGpp synthetase, like the *E. coli* RelA, that also possess (p)ppGpp hydrolase activity characteristic of SpoT (15, 16). In addition to RSH, Gram-positive *Firmicutes* encode one or two (p)ppGpp synthetases (termed RelP and RelQ) that lack the N-terminal Mn^{2+}-dependent hydrolase domain required for (p)ppGpp hydrolysis and the C-terminal regulatory region of RSH enzymes (17–21). Transcriptomic and phenotypic analysis indicated that the bifunctional RSH is the principal enzyme responsible for the rapid accumulation of (p)ppGpp during nutrient limitation but also controls the magnitude and duration of (p)ppGpp accumulation through regulation of (p)ppGpp synthetase activity, hydrolase activity, or both (5, 15, 17–19). However, the specific roles of RelP and RelQ remain elusive.

Previous studies from our group identified and characterized the two enzymes responsible for (p)ppGpp production in *E. faecalis*, the bifunctional RSH and the monofunctional RelQ synthetase; RelP homologues are not found in the genome of enterococci (5, 17). To avoid ambiguity in the nomenclature between the monofunctional RelA of Gram-negative bacteria and the bifunctional enzyme of Gram-positive organisms, we have chosen to adopt the term RSH to refer to the bifunctional enzyme of *E. faecalis*, called RelA in previous publications (5, 17). Characterization of strains lacking *rsh*, *relQ*, or both showed that RSH is responsible for activation of the SR and that (p)ppGpp plays a crucial role in stress survival and virulence (5, 17, 21). A complete lack of (p)ppGpp, as seen in the (p)ppGpp⁰ (Δrsh $\Delta relQ$) strain, led to overall decreased tolerance to vancomycin, reduced survival within macrophages, and attenuated virulence in the *Caenorhabditis elegans* and *Galleria mellonella* models (5, 17). Interestingly, the Δrsh strain, which like the (p)ppGpp⁰ strain is unable to mount the SR, showed enhanced vancomycin tolerance and behaved like the wild-type strain in *in vitro* macrophage survival and invertebrate virulence models.

Despite the relatively long history of (p)ppGpp in bacterial research, substantially less effort has been made to understand its regulatory effect during exponential (balanced) growth. Here, balanced growth represents any physiological condition in which cellular constituents are produced at constant rates relative to one another, leading to a constant rate of cell division. Previous studies have shown that during steady-state growth, *E. coli* produces low basal levels of (p)ppGpp (22, 23). In these studies, a general inverse correlation between basal (p)ppGpp levels and growth rate was established whereby lower growth rates are indicative of higher basal (p)ppGpp pools (23–25). It was later postulated that basal (p)ppGpp pools, despite being at concentrations consider-

ably lower than those observed during the SR, may be high enough to have regulatory effects during balanced growth (26). This lead to the idea that (p)ppGpp acts as a gradient over a range of growth rates rather than a bistable switch to control cellular physiology under nutrient replete ("off") or starvation ("on") conditions (26).

Given the increasing number of studies that report the association of (p)ppGpp with virulence expression, persister cell formation, and other survival-related phenotypes (3, 27–29), a comprehensive understanding of the pathways affected by (p)ppGpp may reveal potential targets for the development of new antimicrobial therapies. To gain a more thorough understanding of the genetic basis through which (p)ppGpp maintains cell homeostasis during balanced growth, we used microarrays to compare the transcriptome of the wild-type strain *E. faecalis* OG1RF to a panel of mutant strains producing different basal levels of (p)ppGpp during exponential growth phase. The transcriptome of a bona fide (p)ppGpp⁰ strain revealed that basal (p)ppGpp pools are essential for a balanced metabolism, providing an additional explanation for the reduced fitness and attenuated virulence of the (p)ppGpp⁰ mutant strain. As recently shown in *Bacillus subtilis* (11), we also found that complete lack of (p)ppGpp led to aberrant regulation of guanosine metabolism characterized by accumulation of intracellular GTP and severe inhibition of growth in the presence of exogenous guanosine. Finally, we expanded our previous observations by showing that the (p)ppGpp-mediated antibiotic tolerance, regardless of the drug target, occurs at (p)ppGpp concentrations that are markedly lower than those achieved during the SR. To the best of our knowledge, this report represents the first global transcriptional comparison of strains with different basal (p)ppGpp levels during balanced growth in any microorganism.

RESULTS

The Δrsh strain has higher basal levels of (p)ppGpp. Among the many phenotypic differences observed between the different (p)ppGpp-deficient strains, the Δrsh strain showed a slow-growth phenotype in rich medium, whereas the $\Delta relQ$ and (p)ppGpp⁰ (Δrsh $\Delta relQ$) strains grew as well as the wild-type strain. Previously, we proposed that the slow growth of the Δrsh strain is a result of the strain's inability to hydrolyze (p)ppGpp synthesized by RelQ, thereby elevating basal (p)ppGpp above wild-type levels (17). To measure basal levels of (p)ppGpp, cultures were uniformly labeled with ^{32}P from early exponential to mid-log growth phase. The basal (p)ppGpp level is defined here as the amount of (p)ppGpp present in nonstressed, logarithmically growing cells. Quantifications of extracted nucleotides separated by thin-layer chromatography (TLC) (Fig. 1B) indicated that basal levels of ppGpp were approximately 4-fold higher in the Δrsh strain than the wild-type strain. The increased ppGpp level in the Δrsh strain was accompanied by an ~40% reduction in GTP. In contrast to ppGpp, pppGpp levels were similar in the wild-type and Δrsh strains. No significant differences in (p)ppGpp pools were observed between wild-type and $\Delta relQ$ strains, and as expected, no (p)ppGpp was detected in the (p)ppGpp⁰ strain.

The transcriptional profile of the Δrsh and Δrsh $\Delta relQ$ strains under balanced growth conditions provides novel insights into the physiological relevance of basal (p)ppGpp pools. Here, microarrays were used to obtain the transcriptional profiles of OG1RF and the Δrsh, $\Delta relQ$, and Δrsh $\Delta relQ$ strains during exponential growth. Given that the *E. faecalis* V583 genome anno-
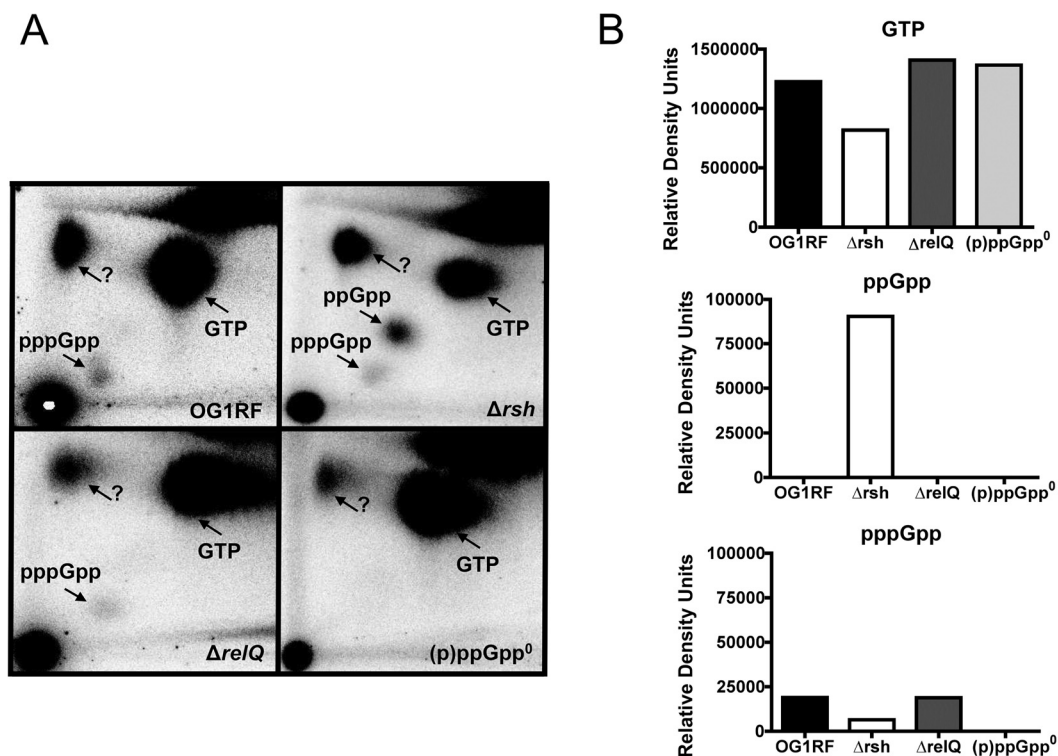
FIG 1 Determination of basal (p)ppGpp levels during nonstressed growth. (A) 2D TLC of [^{32}P]orthophosphate labeled cells. Cells were grown in low-phosphate FMCG to an OD_{600} of 0.25, labeled with 150 μCi ml^{-1} of ^{32}P, and grown to a final optical density (600 nm) of 0.4. The identity of the spot appearing at the top left quadrant of each TLC plate is unknown. (B) Fold change of guanine nucleotide pools compared to the wild-type from 1D TLC separation of ^{32}P-labeled cell extracts. GTP, ppGpp, and pppGpp spots were quantified using a phosphorimager.

tation (30) has been widely used in the literature, we adopted the same gene designation in tables depicting the microarray data. However, genes present in the OG1RF genome but absent in V583 are presented with the original OG1RF designations (31).

At an assigned *P* value of ≤0.001 and a 2-fold cutoff, 51 genes in the Δ*rsh* strain, 17 genes in the Δ*relQ* strain, and 246 genes in the Δ*rsh* Δ*relQ* [(p)ppGpp⁰] strain were differentially expressed compared to the wild-type strain. The complete list of these genes is shown in Table S1 in the supplemental material. A subset of these genes (*n* = 7) was selected for real-time quantitative RT-PCR validation, and all results were consistent with the expression trends observed in the microarrays (see Fig. S1 and Table S2 in the supplemental material). The small number of genes found to be differentially expressed in the Δ*relQ* strain is in agreement with the nearly identical basal levels of (p)ppGpp in this strain and the wild type (Fig. 1). Conversely, a much larger number of genes were differentially expressed in the Δ*rsh* and (p)ppGpp⁰ strains, which have 4-fold-higher basal (p)ppGpp levels and no (p)ppGpp, respectively. Among the genes that were differentially transcribed in the Δ*rsh* strain, 60.8% were upregulated and 39.2% were downregulated. Most notable among the downregulated genes were those involved in nucleotide metabolism, including those encoding nucleoside diphosphate kinase (*ndk*) and GMP reductase (*guaC*). Among the genes activated in the Δ*rsh* strain, a subset correspond to *de novo* pyrimidine biosynthesis (*nrdG*, *nrdD*, *pyrDII*, *pyrB*, *pyrDB*, *pyrE*, *purA*, *pyrC*, and *carB*), suggesting that elevated basal levels of (p)ppGpp interfere with pyrimidine metabolism.

The most prominent differences were observed in the transcriptome of the (p)ppGpp⁰ strain. Remarkably, the overwhelming majority of the differentially expressed genes in this strain were activated (92.6%). A closer evaluation of these genes revealed a dramatic upregulation of genes associated with energy generation, in particular, genes involved in pyruvate production from alternative carbon sources (Fig. 2; also, see Table S1 in the supplemental material). This is surprising, as the cells were grown in a defined but complete medium containing 10 mM glucose, which is sufficient to repress alternate carbon metabolism pathways (32). For example, many genes (*n* = 35) of the various phosphoenolpyruvate:sugar phosphotransferase systems (PTS), the major sugar transport systems at low carbohydrate concentrations, were activated. Likewise, all 13 genes encompassing the *citCL* locus, which is involved in citrate transport and metabolism, were highly induced (ranging from 27- to 134-fold induction) as well as the genes encoding glycerol-3-phosphate oxidase (*glpO*) and glycerol uptake protein (*glpF*), involved in the GlpK pathway of glycerol metabolism (33). Three genes involved in serine degradation (*serS1*, *sdhA-1* and *sdhB-1*), which convert serine into pyruvate, were also highly induced (≥66-fold induction). Finally, the gene encoding the catabolite control protein CcpA, which is responsible for carbon catabolite repression (CCR), was induced 3.2-fold. Among the few repressed genes in the (p)ppGpp⁰ strain (7.4%), a subset are involved in purine metabolism and salvage pathways, including GMP reductase (*guaC*), guanine deaminase (*guaD*), a putative xanthine/uracil permease, IMP cyclohydrolase (*purH*), and adenylosuccinate synthase (*purA*).
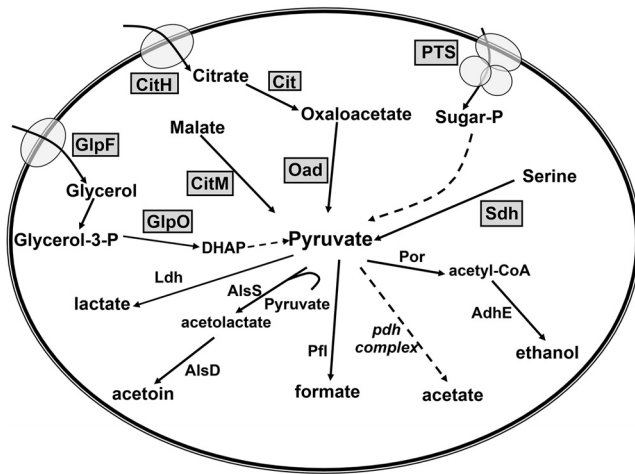
FIG 2 Genes and pathways induced in the (p)ppGpp⁰ strain that lead to the production of pyruvate and heterolactic fermentation products derived from pyruvate in *E. faecalis*. Shaded pathways or proteins specify activated genes detected from microarray analysis. Proteins and protein complexes responsible for the chemical conversion of pyruvate into the five different fermentation end products are in bold but were not detected in microarray comparisons. Dashed lines represent multistep processes. Oad, oxaloacetate dehydrogenase complex; Cit, citrate lyase complex; CitH, citrate transporter; CitM, malate dehydrogenase; Sdh, L-serine dehydratase complex; GlpF, glycerol permease; GlpO, glycerol phosphate oxidase.

The fermentative profile of the (p)ppGpp⁰ strain supports the altered transcriptome. As a typical lactic acid bacterium, *E. faecalis* usually exhibits homolactic fermentation. However, environmental changes, including changes in oxygen availability, pH, and carbon source, can rapidly trigger a switch from homo-

lactic to mixed-acid (heterolactic) fermentation (34). The major end products from heterolactic fermentation include lactate, acetate, formate, acetoin, and ethanol. To investigate whether the transcriptional activation of alternate carbon and energy metabolism genes in the (p)ppGpp⁰ strain is manifested at the physiological level, we compared the intracellular concentration of pyruvate as well as the production of lactate, ethanol, formate, and acetoin secreted into the growth medium between wild-type and (p)ppGpp⁰ strains. We also attempted to measure acetate production, but even with the removal of exogenous acetate, the chemically defined FMC medium was incompatible with the enzymatic assay, leading to high background readings. Despite the transcriptional induction of genes involved in different pathways linked to pyruvate production, the intracellular pyruvate levels of the (p)ppGpp⁰ strain were comparable to those observed in OG1RF (Fig. 3A). However, the (p)ppGpp⁰ strain produced less lactate than OG1RF (e.g., an 11% decrease at an optical density at 600 nm [OD_{600}] of 0.7; $P \leq 0.0001$) and produced more acetoin, formate, and ethanol (Fig. 3B to E). The relatively small total amounts of formate produced [e.g., 2.4% of the total lactate produced at an OD_{600} of 0.7 for the (p)ppGpp⁰ strain] and the marginal difference in ethanol production between OG1RF and the (p)ppGpp⁰ strain (e.g., 4.6% at an OD_{600} of 0.7) is likely to have little, if any, impact on cell physiology. However, the increased production of acetoin (105% increase at an OD_{600} of 0.7; $P \leq 0.0001$) coupled with the reduced production of lactate observed in the (p)ppGpp⁰ strain is more likely to have biological implications, as acetoin is a nonacidic fermentative end product. To assess this possibility, the pH of culture supernatants from wild-type and (p)ppGpp⁰ strains was measured over the different growth phases. In agreement with our metabolite analysis, the wild-type strain was able to reduce the
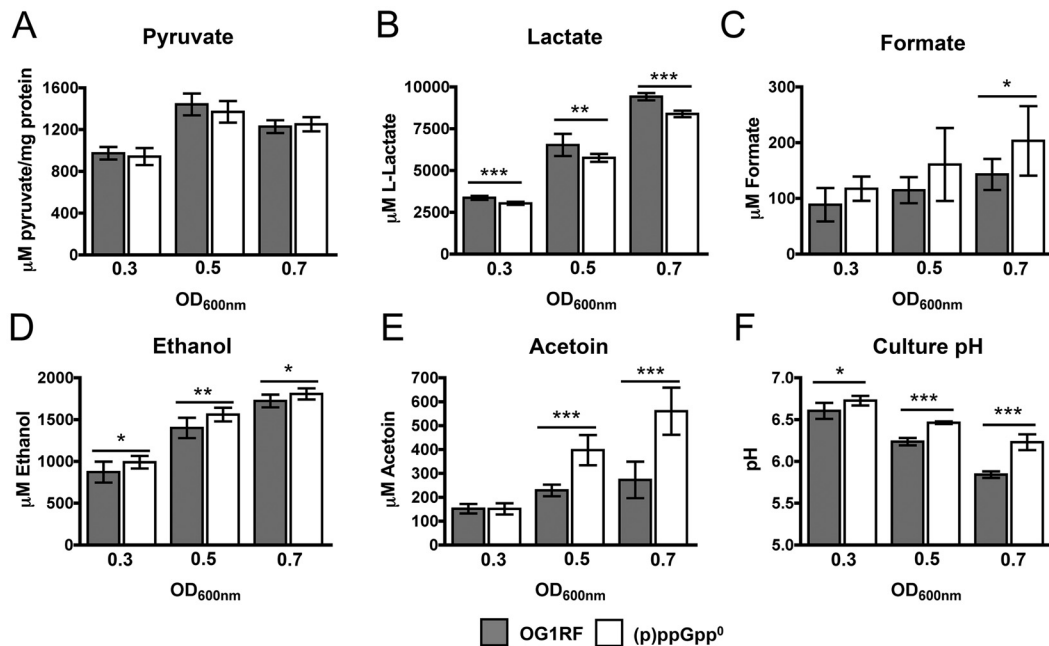
FIG 3 Metabolic profile of wild-type OG1RF and (p)ppGpp⁰ strains. The soluble fraction of whole-cell lysates (for pyruvate measurements) or culture supernatants (for fermentation end products) from *E. faecalis* grown in FMCG were harvested by centrifugation at the indicated optical densities (600 nm) and used to determine the concentrations of pyruvate (A), lactate (B), formate (C), ethanol (D), and acetoin (E) and the culture pH (F). For all assays, $n = 6$ (*, $P < 0.032$; **, $P < 0.005$; ***, $P < 0.0001$).

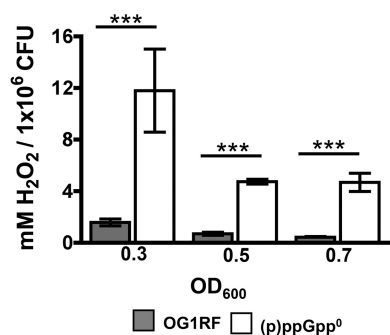**FIG 4** Enhanced H_2O_2 production by the (p)ppGpp^0 strain. Cells of *E. faecalis* OG1RF and (p)ppGpp^0 strains grown in FMCG were harvested at the indicated optical densities and washed in PBS buffer. The washed cell suspension was mixed with an equal volume of buffer to determine H_2O_2 production over a 30-min incubation period. For all assays, $n = 9$ (*, $P < 0.0001$).

external pH to values significantly lower than those achieved by the (p)ppGpp^0 strain (Fig. 3F). Collectively, these results serve to validate the microarray results and suggest that, to maintain pyruvate homeostasis, the (p)ppGpp^0 strain switches from a predominant homolactic fermentation to heterolactic fermentation.

The (p)ppGpp^0 strain produces high levels of H_2O_2. Catabolic control, or the ability to regulate the rate and direction of carbon flow, is important for balancing proliferative capacity with the damaging effects of metabolic by-products, such as reactive oxygen species (ROS) (35). *Enterococcus faecalis* is a potent producer of ROS, including H_2O_2 and superoxide, which are by-products of aerobic glycerol metabolism and the interaction of respiratory chain semiquinone radicals with oxygen (36, 37). At

neutral or low pH, like those in our culture media, H_2O_2 can also rapidly form (8×10^4 M^{-1} s^{-1}) from the spontaneous dismutation of superoxide resulting from the random interaction of two superoxide molecules (38). We compared the production of H_2O_2 between the wild-type OG1RF and (p)ppGpp^0 strains. The (p)ppGpp^0 cells produced at least 6.8-fold more H_2O_2 than the wild type at early log, mid-log, and late log growth phases (Fig. 4). This increased H_2O_2 production further suggests that the (p)ppGpp^0 strain is unable to maintain a balanced metabolism.

Lack of (p)ppGpp disrupts GTP homeostasis. Recently, (p)ppGpp was shown to directly inhibit multiple enzymes involved in GTP synthesis, and disruption of GTP homeostasis in a *B. subtilis* (p)ppGpp^0 strain resulted in metabolic changes that negatively affected cell viability, even in the absence of starvation (11). Addition of exogenous guanosine to the *B. subtilis* (p)ppGpp^0 strain, which is converted to GTP via the salvage pathway, dramatically increases GTP levels, suggesting that (p)ppGpp maintains GTP homeostasis via negative feedback control (11). As demonstrated in *B. subtilis*, the hypoxanthine-guanine phosphoribosyltransferase (HprT) homologue from *E. faecalis* was also specifically inhibited by pppGpp in a dosage-dependent manner with a 50% inhibitory concentration (IC_{50}) of 89.8 ± 10.49 μM (Fig. 5A, top). Although guanylate kinase (Gmk) was inhibited by pppGpp with an IC_{50} of 461.9 ± 106.4 μM (data not shown), this was nonspecific, as GTP was able to inhibit Gmk with an efficiency similar to that of pppGpp (Fig. 5A, bottom). To assess whether (p)ppGpp also exerts posttranscriptional control over GTP synthesis *in vivo*, we investigated the effects of exogenous guanosine on the wild-type and (p)ppGpp-defective strains. Similar to what was seen with *B. subtilis*, addition of guanosine resulted in a sharp
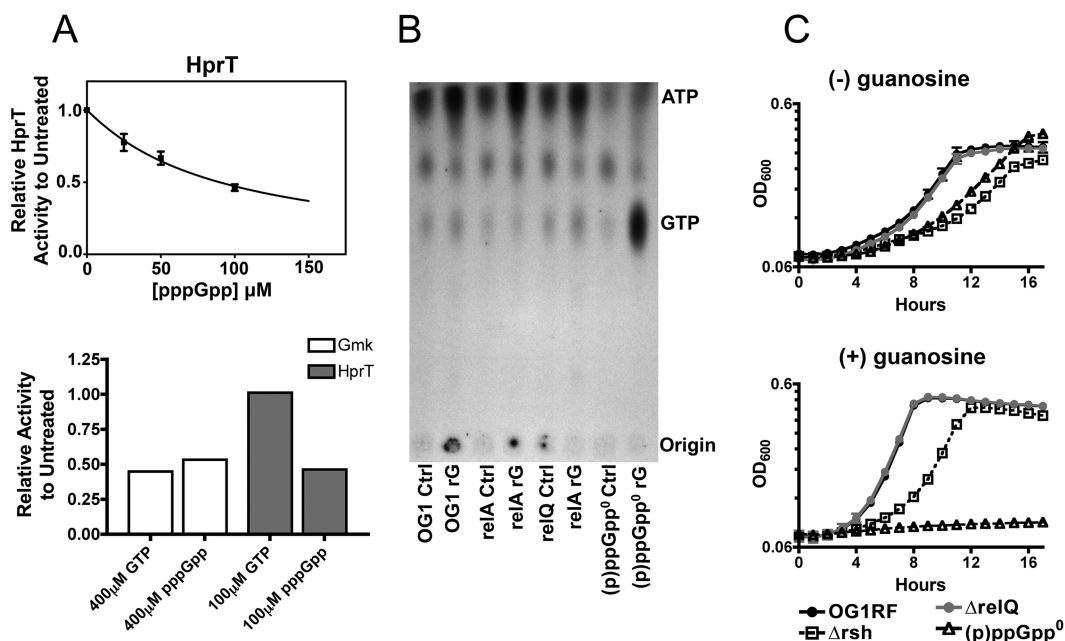

FIG 5 Dysregulation of guanosine metabolism in the (p)ppGpp^0 strain. (A) (Top) HprT inhibition by increasing concentrations of pppGpp *in vitro*. Error bars represent standard errors of three independent experiments. (Bottom) Relative enzymatic activity of HprT and Gmk in the presence of GTP or pppGpp. (B) TLC of ^{32}P-labeled cells showing GTP accumulation in the presence of exogenous guanosine. Cells were grown in FMCG lacking nucleobase supplementation to an OD_{600} of 0.3, labeled with 150 μCi ml^{-1} of ^{32}P, and treated with 2 mM guanosine (rG) for 15 min. Control (Ctrl) samples were not treated with guanosine. (C) Growth inhibition of the (p)ppGpp^0 strain caused by addition of excess guanosine. Cells were grown to early log phase in complete FMCG and diluted into FMCG lacking exogenous nucleobases supplemented with 1 mM guanosine ($n = 3$).
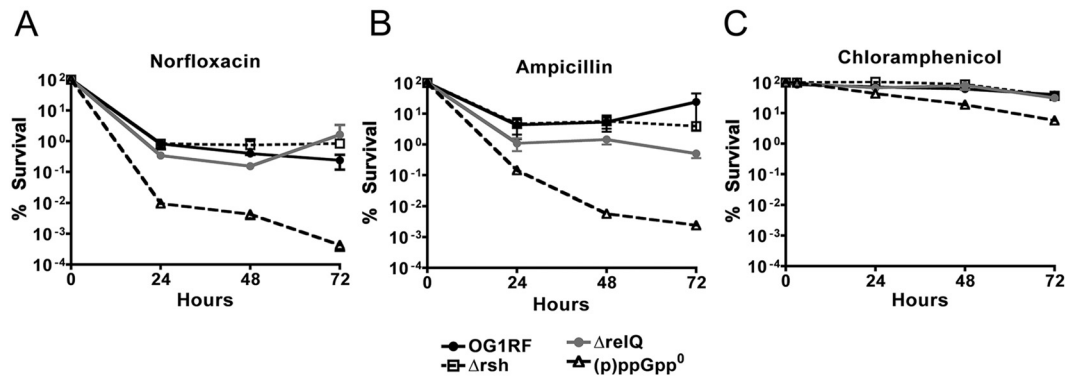
FIG 6 Antibiotic survival of OG1RF, Δ*rsh*, Δ*relQ*, and (p)ppGpp0 strains. Exponentially grown cultures were diluted in fresh FMCG to 5×10^6 to 1×10^7 CFU ml^{-1}, and cell survival after addition of ampicillin ($8 \mu g$ ml^{-1}) (A), norfloxacin ($64 \mu g$ ml^{-1}) (B), or chloramphenicol ($16 \mu g$ ml^{-1}) (C) was monitored over time.

increase in GTP levels in the (p)ppGpp^0 strain, whereas GTP levels remained constant in the wild-type, Δ*rsh*, and Δ*relQ* strains (Fig. 5B). As an apparent result of GTP accumulation, growth of the (p)ppGpp^0 strain was completely inhibited by as little as 1 mM guanosine (Fig. 5C). In contrast with what was seen with *B. subtilis* (11), no significant effect on cell viability was observed in the (p)ppGpp^0 strain following exposure to exogenous guanosine (data not shown). These results serve to highlight another crucial function of (p)ppGpp, that seems to be separate from the SR activation, in balancing guanosine metabolism with cellular demands for macromolecular biosynthesis and energy generation.

(p)ppGpp-mediated antibiotic protection occurs independently of SR activation. Although the association of (p)ppGpp metabolism with antibiotic tolerance has been known for several years (39, 40), recent studies suggested that activation of the SR is central to the formation of persister cells in Gram-negative bacteria (28, 41). Previously, we showed that the *E. faecalis* (p)ppGpp^0 strain (Δ*rsh* Δ*relQ*) was significantly more sensitive to vancomycin, whereas the Δ*rsh* strain showed increased survival rates (17). Here, we expanded this initial finding by conducting time-kill kinetics studies with two additional bactericidal drugs: ampicillin (β-lactam) and norfloxacin (DNA gyrase inhibitor) (Fig. 6). In both cases, the survival rates of the Δ*relQ* strain were not statistically different from those of the wild type. However, the (p)ppGpp^0 strain was killed more rapidly ($P \leq 0.001$). Despite the fact that the Δ*rsh* strain has only RelQ as a source of (p)ppGpp synthesis and is unable to activate the SR (5), this strain showed rates of survival against ampicillin or norfloxacin similar to those of the wild-type strain. To verify that the survival differences among strains were not due to differences in long-term viability, cells were exposed to the bacteriostatic antibiotic chloramphenicol. Despite a small reduction in the viability of the (p)ppGpp^0 strain after 48 h, the differences observed were not statistically significant (Fig. 6C). These results indicate that, in *E. faecalis*, (p)ppGpp-mediated protection occurs at levels that are well below those needed to trigger the SR.

DISCUSSION

Lack of RSH results in constitutively high levels of (p)ppGpp. Previously, we demonstrated that inactivation of the bifunctional RSH resulted in a slow-growth phenotype, a characteristic that could be rescued with the simultaneous inactivation of RelQ (17). Identical observations have been made in *Streptococcus mutans*

and *B. subtilis*, which encode two small (p)ppGpp synthetases, indicating that the slow growth of *rsh* mutants is associated with reduced intracellular GTP due to constitutive production of (p)ppGpp by one (in the case of *E. faecalis*) or two monofunctional (p)ppGpp-synthetases (18, 19, 42, 43). In the present study, by extending the duration of isotopic labeling under nonstringent conditions, we acquired unequivocal evidence that the Δ*rsh* strain accumulates higher basal levels of (p)ppGpp at the expense of intracellular GTP. Interestingly, the differences in (p)ppGpp levels were restricted to ppGpp, not pppGpp. This observation may have important biological implications, as studies conducted with *E. coli* revealed that ppGpp is a more effective regulator (~10 times more potent than pppGpp) for several SR-controlled phenomena (44). Previous studies have shown that RelQ paralogs can efficiently utilize GDP or GTP to synthesize, respectively, ppGpp and pppGpp, although no substrate preference experiments have been conducted (19, 45). The accumulation of ppGpp in the Δ*rsh* strain may be an indication that RelQ preferentially utilizes GDP over GTP. Another possible explanation for the ppGpp accumulation in Δ*rsh* is that pppGpp produced from GTP is unstable and rapidly degraded into ppGpp (46). In Gram-negative bacteria, guanosine pentaphosphatases (Gpp) are responsible for the conversion of pppGpp to ppGpp *in vivo*, although alternate pathways for (p)ppGpp degradation have been shown *in vitro* (47, 48). However, no homologues of *gpp* have been identified in *E. faecalis* and closely related Gram-positive bacteria. At the present time, the reasons for the accumulation of ppGpp, but not of pppGpp, in the Δ*rsh* strain remain undetermined. Work is under way to investigate the possibility that the *E. faecalis* RelQ preferentially utilizes GDP over GTP.

The activation of alternate carbon and energy metabolism genes in the (p)ppGpp^0 strain may be linked to CCR alleviation. The key finding from the microarray analysis was the observation that a complete lack of (p)ppGpp caused large-scale transcriptional alterations during balanced growth. A closer examination of these transcriptional alterations showed that genes involved in the production of pyruvate via multiple pathways, including glycolysis, secondary-carbon-source metabolism (citrate, glycerol, and malate), and serine degradation, were highly induced in the (p)ppGpp^0 strain. Although we did not observe increased production of pyruvate in the (p)ppGpp^0 strain, the ability of this strain to maintain pyruvate homeostasis is likely linked to enhanced ace-

toin production, as two molecules of pyruvate are consumed for every molecule of acetoin generated. Additionally, the acetolactate synthase (ALS) enzyme has a lower K_m for pyruvate than other competing fermentative enzymes. Hence, acetoin production is favored when intracellular pyruvate is abundant.

Among the energy generation pathways transcriptionally induced in the (p)ppGpp^0 strain were multiple PTS genes, two divergent citrate metabolism operons, and glycerol uptake and metabolism genes. Notably, these metabolic pathways are known to be under carbon catabolite regulation (CCR), mediated by CcpA, in different Gram-positive bacteria (49–51). CcpA is a global regulator of carbon metabolism, either positive or negative, and its activity is stimulated through interactions with PTS enzymes and by the availability of the glycolytic intermediates glucose-6-phosphate and fructose-1,6-bisphosphate (FBP) (52). Thus, metabolic alterations observed in the (p)ppGpp^0 strain may serve as an explanation for CCR alleviation. Moreover, when compared to the parent strain, transcription of the ccpA gene was also induced. While the concomitant upregulation of *ccpA* with CcpA-regulated genes may appear counterintuitive, this likely represents an attempt by the cell to constrain alternate carbon metabolism, diverting it back to the utilization of preferential carbon sources such as glucose. The upregulation of alternate carbon catabolism pathways suggests that the (p)ppGpp^0 strain is unable to accurately sense external and internal metabolic cues.

The enhanced generation of H_2O_2 may help explain several phenotypes of the (p)ppGpp^0 strain. The linkage of enhanced ROS generation with the (p)ppGpp^0 strain phenotypes is of particular interest due to the strain's enhanced susceptibility to bactericidal antibiotics, reduced survival within murine macrophages, and attenuated virulence in two invertebrate models (5, 17). In every case, a negative correlation between ROS generation and bacterial viability appears to exist, although the model proposing endogenous ROS generation as a common killing mechanism of bactericidal antibiotics was recently challenged (53–55). In line with the transcriptome analysis that suggested enhanced metabolic flux, an indicator of increased ROS generation (35), we detected a >5-fold increase in H_2O_2 production by the (p)ppGpp^0 strain during exponential growth. As a potential protective mechanism to compensate for increased ROS production, the transcription of several oxidative stress genes was induced in the (p)ppGpp^0 strain, including NADH peroxidase, peroxiredoxin, thioredoxin disulfide reductase, and ferrodoxin reductase (see Table S1 in the supplemental material). Thus, while the (p)ppGpp^0 strain appears to be able to cope with intrinsically higher rates of intracellular ROS under favorable growth conditions, this strain may be at the limit of its antioxidant capacity and is, therefore, more susceptible to exogenous ROS exposure.

Regulation of GTP pools by (p)ppGpp is central to adaptation and survival. Recent advances defining the direct regulation of GTP homeostasis by (p)ppGpp in *B. subtilis* and, more importantly, showing that GTP depletion enhances stress survival independently of (p)ppGpp have provided new mechanistic insight onto the underlying causes of the often divergent phenotypes in our two SR-defective mutants (the Δ*rsh* and Δ*rsh* Δ*relQ* strains). In accordance with results for *B. subtilis* (11), we observed that (p)ppGpp directly controls GTP homeostasis in *E. faecalis*. Specifically, HprT and Gmk were inhibited by pppGpp (IC$_{50}$ ~ 100 μM for HprT and 400 μM for Gmk) at physiologically relevant levels, as (p)ppGpp levels can reach low-millimolar levels during a de-

veloped stringent response in other bacteria (56). At an concentration equivalent to that of pppGpp, GTP had no effects on HprT activity but similar effects on Gmk activity, indicating that pppGpp inhibition is specific to HprT but nonspecific for Gmk. Based on our results, pppGpp appears to be a more potent and specific inhibitor for HprT than Gmk, suggesting that regulation of HprT by pppGpp is probably the major mechanism for maintaining GTP homeostasis in *E. faecalis*. In addition, we observed GTP accumulation and severe growth inhibition when the (p)ppGpp^0 strain, but not the Δ*rsh* strain, was cultured in the presence of excess guanosine. Thus, it is very likely that the different, often opposing, phenotypes of Δ*rsh* and (p)ppGpp^0 strains result from differences in GTP levels (low and high GTP, respectively) in these strains. Changes in GTP pools will directly affect the activity of the metabolic regulator CodY, which senses both carbon and nitrogen availability by responding to branched-chain amino acids and GTP levels, creating a complex and integrated system to control nutrient acquisition and utilization in Gram-positive bacteria (57). The opposing 4-fold-elevated and no basal (p)ppGpp levels in Δ*rsh* and (p)ppGpp^0 strains may then correlate to reduced and high CodY activity, respectively. In addition to interference with CodY activity, the guanine energy charge (GTP/GDP ratio) could also play a more direct role in the phenotypes associated with the (p)ppGpp^0 strain. GTP is a key component of anabolic cellular processes, including synthesis of stable RNAs, polyamine synthesis, and all three stages of translation (8, 58).

The relationship between (p)ppGpp and antibiotic tolerance occurs at levels that do not trigger the classic SR. In Gram-negative bacteria, recent studies proposed that (p)ppGpp participates in antibiotic tolerance by (i) controlling ROS metabolism and activating detoxification enzymes (41, 59), (ii) functioning as an unconventional metabolic toxin-antitoxin (TA) module (28), and (iii) potentiating the action of the HipAB TA module (60). Although we have a relatively good understanding of the underlying mechanisms by which (p)ppGpp modulates antimicrobial tolerance in Gram-negative bacteria, much less is known about the process in Gram-positive species. Interestingly, two independent whole-genome sequencing studies identified point mutations in the *rsh* gene of *Staphylococcus aureus* isolates, which resulted in increased accumulation of (p)ppGpp, as being directly responsible for the emergence of antibiotic-tolerant (persister) cells (61, 62). Previously, we showed that a complete lack of (p)ppGpp, as seen in the (p)ppGpp^0 strain, resulted in increased sensitivity to vancomycin (17). However, the Δ*rsh* strain showed enhanced tolerance to vancomycin (17). By expanding our previous observation to other bactericidal antibiotics, we showed here that only the (p)ppGpp^0 strain, not the Δ*rsh* strain, displayed enhanced sensitivity to bactericidal antibiotics. Collectively, the differences in antibiotic tolerance observed between Δ*rsh* and (p)ppGpp^0 strains clearly indicate that (p)ppGpp is central for antibiotic tolerance but that this phenomenon occurs at (p)ppGpp concentrations that are much lower than those necessary to activate the SR. While the SR was abolished in both Δ*rsh* and (p)ppGpp^0 strains (5), the differences in basal (p)ppGpp and GTP pools between these two strains appear to be directly associated with antibiotic tolerance. Work is under way to understand how small changes in intracellular guanine nucleotide pools, mediated by RelQ, enhance *E. faecalis* tolerance to bactericidal antibiotics.

Concluding remarks. Collectively, our microarray data and supporting physiological assays indicate that the (p)ppGpp^0 strain cannot control the pace and direction of carbon flow and, as a result, is unable to sense and respond to environment changes accordingly. As a consequence, a strain unable to synthesize (p)ppGpp may have uncontrolled consumption of energy stores, unbalanced NAD$^+$/NADH ratios, increased ROS generation due to increased metabolic activity, and unbalanced GTP homeostasis. All of these factors combined likely reduce the long-term fitness of the cells.

Since the identification of (p)ppGpp more than four decades ago, mounting evidence has shown that activation of the SR is central for controlling responses that promote cell survival during adverse conditions. In the past few years, stringent control and (p)ppGpp metabolism have been, once again, the subject of intense research. The picture emerging from these most recent investigations is that bacteria utilize (p)ppGpp in many different ways, and that the paradigm for Gram-negative organisms does not apply fully to Gram-positive bacteria. In this study, we provided new evidence that the role of (p)ppGpp in the physiology of Gram-positive bacteria goes well beyond activation of the SR.

MATERIALS AND METHODS

Bacterial strains and growth conditions. *E. faecalis* OG1RF and its derivatives JAL1 (Δrsh, formerly $\Delta relA$), JAL2 ($\Delta relQ$), and JAL3 ($\Delta rsh \Delta relQ$, formerly $\Delta relA \Delta relQ$) strains have been previously described (17). For microarray analysis, cells were grown at 37°C in the chemically defined medium FMC (63) containing all amino acids, eight vitamins, three nucleobases (adenine, guanine, and uracil), and salts and supplemented with 10 mM glucose (FMCG) to an optical density at 600 nm (OD$_{600}$) of 0.3. To assess the effects of excess guanosine on growth, cells were cultured in complete FMCG until the OD$_{600}$ was 0.3 and diluted 1:100 into FMCG lacking nucleobases but supplemented with increasing concentrations of guanosine. For detection of (p)ppGpp, overnight cultures were diluted in fresh FMCG containing reduced phosphate (8.6 mM) (17), grown to an OD$_{600}$ of ~0.25, and labeled with 150 μCi ml^{-1} of carrier-free [^{32}P]orthophosphate (PerkinElmer, Waltham, MA) until each culture reached an OD$_{600}$ of 0.4 (~50 min for the OG1RF and $\Delta relQ$ strains, ~55 min for the $\Delta rsh \Delta relQ$ strain, and ~70 min for the Δrsh strain). For GTP accumulation experiments, cells were grown in low-phosphate FMCG lacking nucleotide, nucleoside, or nucleobase supplementation to an OD$_{600}$ of 0.3 and labeled with 150 μCi ml^{-1} of ^{32}P along with the simultaneous addition of 2 mM guanosine to the growth medium for 15 min. Control samples received no exogenous guanosine.

Detection of intracellular guanine nucleotides. For (p)ppGpp and GTP detection, nucleotides were extracted by adding an equal volume of 13 M formic acid followed by two freeze-thaw cycles in a dry-ice--ethanol bath. Acid extracts were centrifuged, and the supernatants were spotted onto polyethyleneimine cellulose plates (J. T. Backer/Avantor Performance Materials, Center Valley, PA). For two-dimensional (2D) TLC separation, samples were first separated in 3.3 M ammonium formate, 4.2% boric acid (pH 7.0 with NH$_4$OH), followed by a second-dimension separation in 1.5 M KH$_2$PO$_4$ (pH 3.4). TLC plates were desalted by soaking for 5 min in methanol before and after each run. (p)ppGpp and GTP pools were quantified using a phosphorimager (molecular imager FX; Bio-Rad, Hercules, CA).

RNA extraction. To isolate RNA from *E. faecalis*, cells were harvested by centrifugation at 4°C and then treated with the RNA Protect reagent (Qiagen, Inc., Chatsworth, CA). Total RNA was isolated from homogenized *E. faecalis* cells by the hot acid-phenol method as described previously (64). RNA pellets were resuspended in nuclease-free H$_2$O and treated with DNase I (Ambion/Life Technologies) at 37°C for 30 min. The RNA was purified again using the RNeasy minikit (Qiagen), including a second on-column DNase treatment that was performed as recom-

mended by the supplier. RNA concentrations were determined using a NanoDrop ND-1000 spectrophotometer (Thermo, Fisher Scientific, Waltham, MA).

Microarray experiments. Transcriptome analysis was performed using the *E. faecalis* microarrays provided by the J. Craig Venter Institute Pathogen Functional Genomics Resource Center (PFGRC). Additional details regarding the arrays can be found at http://pfgrc.jcvi.org/index .php/microarray/array_description/enterococcus_faecalis/version1 .html. Microarray experiments were carried out as previously described (5).

Real-time quantitative PCR. A subset of genes was selected to validate the microarray analysis by real-time quantitative reverse transcription (qRT) PCR. Gene-specific primers (see Table S3 in the supplemental material) were designed using Beacon Designer 2.0 software (Premier Biosoft International). Reverse transcription and real-time reverse transcriptase PCR were carried out on a StepOnePlus real-time PCR system (Life Technologies, Grand Island, NY) according to protocols described elsewhere (64). Student's *t* test was performed to verify significance of the real-time PCR quantifications.

Measurement of intracellular pyruvate and extracellular accumulation of fermentation end products. Intracellular pyruvate levels were determined as previously described (65). Briefly, cells were grown in FMCG to early log phase (OD$_{600}$ = 0.3), mid-log phase (OD$_{600}$ = 0.5), and late log phase (OD$_{600}$ = 0.7), harvested by centrifugation, and washed twice in 50 mM sodium phosphate buffer (pH 6.7). Cell pellets were lysed using a bead beater and centrifuged to remove insoluble matter. In opaque 96-well microtiter plates, 50 μl of soluble lysate was added to 50 μl of reaction buffer containing 100 mM NaPO$_4$ (pH 6.7), 0.2 mM MgSO$_4$, 10 μM FAD, 0.2 mM thiamine pyrophosphate (TPP), 0.2 U ml^{-1} pyruvate oxidase, 0.5 U ml^{-1} horseradish peroxidase (HRP), and 50 μM Amplex UltraRed (Life Technologies). Reaction mixtures were incubated at 37°C for 30 min, and fluorescence was measured by excitation at 470 nm and emission at 590 nm. Pyruvate concentrations were normalized to total cell protein content, determined by bicinchoninic acid (BCA) assay.

Lactic acid, formate, and ethanol were measured using Megazyme enzymatic kits (Megazyme International, Wicklow, Ireland). Assays were conducted according to the manufacturer's protocol using a 96-well plate format. Acetoin production was measured using a Voges-Proskauer test adapted for use in a 96-well plate as described previously (66). For all analyses, cells were grown to early log, mid-log, and late log phase in FMCG as described above. At the respective time points, aliquots were centrifuged for 5 min, and the cell-free culture supernatants were stored on ice, except for aliquots used for pH determination, which were assessed immediately after centrifugation. Before use in fermentative assays, chilled supernatants were removed from ice and allowed to equilibrate to room temperature.

H$_2$O$_2$ measurements. The production of H$_2$O$_2$ was measured using an H$_2$O$_2$-peroxidase assay kit (Life Technologies). Briefly, cells were grown to early log, mid-log, or late log phase in FMCG as described above, harvested by centrifugation, washed once in assay buffer (50 mM Tris-HCl at pH 7.4), and diluted 1:2 in the assay buffer. Reactions were initiated by mixing 50 μl of cell suspension with 50 μl of reaction mix (50 mM Tris-HCl [pH 7.4], 20 μM Amplex UltraRed, and 0.2 U ml^{-1} horseradish peroxidase) in opaque 96-well microtiter plates at 37°C for 30 min. Fluorescence was read in a SpectraMax MX5 reader (Molecular Devices LLC, Sunnyvale, CA) with excitation at 490 nm and emission at 590 nm. To normalize fluorescence by CFU, cells aliquots from each growth phase were serially diluted and plated onto BHI agar for colony enumeration.

Purification and enzymatic assays of HprT and Gmk. The genes encoding Gmk and HprT from *E. faecalis* OG1RF were cloned into pLICTrPC-HA (67) using a ligation-independent cloning technique, and the recombinant plasmids were transformed into *E. coli* BL21(DE3). Cells were grown from a single colony at 37°C in LB supplemented with 100 μg ml^{-1} carbenicillin to an OD$_{600}$ of ~0.6, and isopropyl β-D-1-thiogalactopyranoside was added to a final concentration of 1 mM. Cells

were grown for another 3 h before harvest. Proteins were purified using Ni-NTA spin columns (Qiagen) following the manufacturer's instructions. Protein concentration was determined either by Bradford protein assay (Bio-Rad) or by measuring absorbance at 280 nm using theoretical molar extinction coefficients. Standard protocols for Gmk and HprT enzymatic assays were followed, with minor modifications (11). HprT reactions were performed at 25°C in a 100-μl reaction mix containing 100 mM Tris-HCl (pH 7.4), 1.2 mM MgCl$_2$, 1 mM 5-phosphoribosyl 1-pyrophosphate (PRPP), 50 μM guanine, 20 nM purified HprT enzyme, and various pppGpp concentrations. Reactions were initiated by adding the enzyme and monitored for 10 min by measuring change of absorbance at 257 nm. Gmk reactions were performed at 25°C in a 100-μl reaction mix containing 100 mM Tris-HCl (pH 7.5), 100 mM KCl, 10 mM MgCl$_2$, 4 mM ATP, 1.5 mM phospho(enol)pyruvic acid, 250 μM NADH, 2 U pyruvate kinase (from rabbit muscle; Sigma), 2.64 U L-lactic dehydrogenase (from bovine heart; Sigma), 50 μM GMP, 10 nM purified Gmk, and various pppGpp concentrations. Reactions were initiated by adding GMP and monitored for 10 min by measuring the change in absorbance at 340 nm. Data were fitted into the equation $y = 100\%/[1 + (x/\text{IC}_{50})^S]$, where y is the relative enzyme activity, x is the inhibitor concentration, and S is the slope factor (GraphPad Prism version 5.02 for Windows; GraphPad Software, San Diego, CA). To confirm the specificity of HprT and Gmk inhibition by pppGpp, control reactions were performed using the conditions described above except that GTP was substituted for pppGpp at concentrations approximately equivalent to the IC$_{50}$s of pppGpp (100 μM for HprT and 400 μM for Gmk).

Antibiotic time-kill kinetics. Cultures were grown in FMCG to exponential phase and diluted in fresh FMCG to 5×10^6 to 1×10^7 CFU ml^{-1}. Time-kill studies were initiated by adding ampicillin (8 μg ml^{-1}), norfloxacin (64 μg ml^{-1}), or chloramphenicol (16 μg ml^{-1}), which represents 5 to 10 times the MIC of these antibiotics for the wild-type OG1RF strain. Viable counts were determined by plating cultures on tryptic soy agar (TSA) plates at time zero, immediately before the addition of antibiotic, and then every 24 h following antibiotic exposure.

Microarray data accession number. Microarray data have been deposited in NCBIs Gene Expression Omnibus (GEO; http://www.ncbi.nlm.nih.gov/geo) and are accessible through GEO Series accession number GSE34561.

SUPPLEMENTAL MATERIAL

Supplemental material for this article may be found at http://mbio.asm.org/lookup/suppl/doi:10.1128/mBio.00646-13/-/DCSupplemental.

Figure S1, TIF file, 6.1 MB.
Table S1, PDF file, 0.1 MB.
Table S2, DOCX file, 0.1 MB.
Table S3, DOCX file, 0.1 MB.

ACKNOWLEDGMENTS

REFERENCES

1. **Arias CA, Murray BE.** 2012. The rise of the *Enterococcus*: beyond vancomycin resistance. Nat. Rev. Microbiol. **10**:266–278.
2. **Murray BE.** 1990. The life and times of the *Enterococcus*. Clin. Microbiol. Rev. **3**:46–65.
3. **Potrykus K, Cashel M.** 2008. (p)ppGpp: still magical? Annu. Rev. Microbiol. **62**:35–51.
4. **Lemos JA, Nascimento MM, Lin VK, Abranches J, Burne RA.** 2008. Global regulation by (p)ppGpp and CodY in *Streptococcus mutans*. J. Bacteriol. **190**:5291–5299.
5. **Gaca AO, Abranches J, Kajfasz JK, Lemos JA.** 2012. Global transcriptional analysis of the stringent response in *Enterococcus faecalis*. Microbiology **158**:1994–2004.
6. **Traxler MF, Summers SM, Nguyen HT, Zacharia VM, Hightower GA, Smith JT, Conway T.** 2008. The global, ppGpp-mediated stringent response to amino acid starvation in *Escherichia coli*. Mol. Microbiol. **68**:1128–1148.
7. **Geiger T, Goerke C, Fritz M, Schäfer T, Ohlsen K, Liebeke M, Lalk M, Wolz C.** 2010. Role of the (p)ppGpp synthase RSH, a RelA/SpoT homolog, in stringent response and virulence of *Staphylococcus aureus*. Infect. Immun. **78**:1873–1883.
8. **Krásný L, Gourse RL.** 2004. An alternative strategy for bacterial ribosome synthesis: *Bacillus subtilis* rRNA transcription regulation. EMBO J. **23**:4473–4483.
9. **Vrentas CE, Gaal T, Berkmen MB, Rutherford ST, Haugen SP, Vassylyev DG, Ross W, Gourse RL.** 2008. Still looking for the magic spot: the crystallographically defined binding site for ppGpp on RNA polymerase is unlikely to be responsible for rRNA transcription regulation. J. Mol. Biol. **377**:551–564.
10. **Kuroda A, Murphy H, Cashel M, Kornberg A.** 1997. Guanosine tetra- and pentaphosphate promote accumulation of inorganic polyphosphate in *Escherichia coli*. J. Biol. Chem. **272**:21240–21243.
11. **Kriel A, Bittner AN, Kim SH, Liu K, Tehranchi AK, Zou WY, Rendon S, Chen R, Tu BP, Wang JD.** 2012. Direct regulation of GTP homeostasis by (p)ppGpp: a critical component of viability and stress resistance. Mol. Cell **48**:231–241.
12. **Wang JD, Sanders GM, Grossman AD.** 2007. Nutritional control of elongation of DNA replication by (p)ppGpp. Cell **128**:865–875.
13. **Xiao H, Kalman M, Ikehara K, Zemel S, Glaser G, Cashel M.** 1991. Residual guanosine 3′,5′-bispyrophosphate synthetic activity of *relA* null mutants can be eliminated by *spoT* null mutations. J. Biol. Chem. **266**:5980–5990.
14. **Gentry DR, Cashel M.** 1996. Mutational analysis of the *Escherichia coli* *spoT* gene identifies distinct but overlapping regions involved in ppGpp synthesis and degradation. Mol. Microbiol. **19**:1373–1384.
15. **Mechold U, Cashel M, Steiner K, Gentry D, Malke H.** 1996. Functional analysis of a *relA/spoT* gene homolog from *Streptococcus equisimilis*. J. Bacteriol. **178**:1401–1411.
16. **Mechold U, Murphy H, Brown L, Cashel M.** 2002. Intramolecular regulation of the opposing (p)ppGpp catalytic activities of Rel(Seq), the Rel/Spo enzyme from *Streptococcus equisimilis*. J. Bacteriol. **184**:2878–2888.
17. **Abranches J, Martinez AR, Kajfasz JK, Chávez V, Garsin DA, Lemos JA.** 2009. The molecular alarmone (p)ppGpp mediates stress responses, vancomycin tolerance, and virulence in *Enterococcus faecalis*. J. Bacteriol. **191**:2248–2256.
18. **Lemos JA, Lin VK, Nascimento MM, Abranches J, Burne RA.** 2007. Three gene products govern (p)ppGpp production by *Streptococcus mutans*. Mol. Microbiol. **65**:1568–1581.
19. **Nanamiya H, Kasai K, Nozawa A, Yun CS, Narisawa T, Murakami K, Natori Y, Kawamura F, Tozawa Y.** 2008. Identification and functional analysis of novel (p)ppGpp synthetase genes in *Bacillus subtilis*. Mol. Microbiol. **67**:291–304.
20. **Battesti A, Bouveret E.** 2006. Acyl carrier protein/SpoT interaction, the switch linking SpoT-dependent stress response to fatty acid metabolism. Mol. Microbiol. **62**:1048–1063.
21. **Yan X, Zhao C, Budin-Verneuil A, Hartke A, Rincé A, Gilmore MS, Auffray Y, Pichereau V.** 2009. The (p)ppGpp synthetase RelA contributes to stress adaptation and virulence in *Enterococcus faecalis* V583. Microbiology **155**:3226–3237.
22. **Ryals J, Little R, Bremer H.** 1982. Control of rRNA and tRNA syntheses in *Escherichia coli* by guanosine tetraphosphate. J. Bacteriol. **151**:1261–1268.
23. **Sarubbi E, Rudd KE, Cashel M.** 1988. Basal ppGpp level adjustment shown by new *spoT* mutants affect steady state growth rates and *rrnA* ribosomal promoter regulation in *Escherichia coli*. Mol. Gen. Genet. **213**:214–222.
24. **Lazzarini RA, Cashel M, Gallant J.** 1971. On the regulation of guanosine tetraphosphate levels in stringent and relaxed strains of *Escherichia coli*. J. Biol. Chem. **246**:4381–4385.
25. **Sokawa Y, Sokawa J, Kaziro Y.** 1975. Regulation of stable RNA synthesis and ppGpp levels in growing cells of *Escherichia coli*. Cell **5**:69–74.
26. **Cashel M, Gentry D, Hernandez VJ, Vinella D.** 1996. The stringent response, p 1458–1496. *In* Neidhardt FC, Ingraham JL, Low BK, Magasanik B, Schaechter M, Umbarger HE (ed), *Escherichia coli* and *Salmonella typhimurium*: cellular and molecular biology, 2nd ed. ASM Press, Washington, DC.

27. Dalebroux ZD, Yagi BF, Sahr T, Buchrieser C, Swanson MS. 2010. Distinct roles of ppGpp and DksA in *Legionella pneumophila* differentiation. Mol. Microbiol. **76**:200–219.

28. Amato SM, Orman MA, Brynildsen MP. 2013. Metabolic control of persister formation in *Escherichia coli*. Mol. Cell **50**:475–487.

29. Gerdes K, Maisonneuve E. 2012. Bacterial persistence and toxin-antitoxin loci. Annu. Rev. Microbiol. **66**:103–123.

30. Paulsen IT, Banerjei L, Myers GS, Nelson KE, Seshadri R, Read TD, Fouts DE, Eisen JA, Gill SR, Heidelberg JF, Tettelin H, Dodson RJ, Umayam L, Brinkac L, Beanan M, Daugherty S, DeBoy RT, Durkin S, Kolonay J, Madupu R, Nelson W, Vamathevan J, Tran B, Upton J, Hansen T, Shetty J, Khouri H, Utterback T, Radune D, Ketchum KA, Dougherty BA, Fraser CM. 2003. Role of mobile DNA in the evolution of vancomycin-resistant *Enterococcus faecalis*. Science **299**:2071–2074.

31. Bourgogne A, Garsin DA, Qin X, Singh KV, Sillanpaa J, Yerrapragada S, Ding Y, Dugan-Rocha S, Buhay C, Shen H, Chen G, Williams G, Muzny D, Maadani A, Fox KA, Gioia J, Chen L, Shang Y, Arias CA, Nallapareddy SR, Zhao M, Prakash VP, Chowdhury S, Jiang H, Gibbs RA, Murray BE, Highlander SK, Weinstock GM. 2008. Large scale variation in *Enterococcus faecalis* illustrated by the genome analysis of strain OG1RF. Genome Biol. **9**:R110.

32. Seidl K, Müller S, François P, Kriebitzsch C, Schrenzel J, Engelmann S, Bischoff M, Berger-Bächi B. 2009. Effect of a glucose impulse on the CcpA regulon in *Staphylococcus aureus*. BMC Microbiol. **9**:95.

33. Bizzini A, Zhao C, Budin-Verneuil A, Sauvageot N, Giard JC, Auffray Y, Hartke A. 2010. Glycerol is metabolized in a complex and strain-dependent manner in *Enterococcus faecalis*. J. Bacteriol. **192**:779–785.

34. Thomas TD, Ellwood DC, Longyear VM. 1979. Change from homo- to heterolactic fermentation by *Streptococcus lactis* resulting from glucose limitation in anaerobic chemostat cultures. J. Bacteriol. **138**:109–117.

35. Nyström T, Larsson C, Gustafsson L. 1996. Bacterial defense against aging: role of the *Escherichia coli* ArcA regulator in gene expression, readjusted energy flux and survival during stasis. EMBO J. **15**:3219–3228.

36. Pugh SY, Knowles CJ. 1982. Growth of *Streptococcus faecalis* var. zymogenes on glycerol: the effect of aerobic and anaerobic growth in the presence and absence of haematin on enzyme synthesis. J. Gen. Microbiol. **128**:1009–1017.

37. Huycke MM, Moore D, Joyce W, Wise P, Shepard L, Kotake Y, Gilmore MS. 2001. Extracellular superoxide production by *Enterococcus faecalis* requires demethylmenaquinone and is attenuated by functional terminal quinol oxidases. Mol. Microbiol. **42**:729–740.

38. Fridovich I. 1983. Superoxide radical: an endogenous toxicant. Annu. Rev. Pharmacol. Toxicol. **23**:239–257.

39. Rodionov DG, Ishiguro EE. 1995. Direct correlation between overproduction of guanosine 3′,5′-bispyrophosphate (ppGpp) and penicillin tolerance in *Escherichia coli*. J. Bacteriol. **177**:4224–4229.

40. Kusser W, Ishiguro EE. 1987. Suppression of mutations conferring penicillin tolerance by interference with the stringent control mechanism of *Escherichia coli*. J. Bacteriol. **169**:4396–4398.

41. Khakimova M, Ahlgren HG, Harrison JJ, English AM, Nguyen D. 2013. The stringent response controls catalases in *Pseudomonas aeruginosa* and is required for hydrogen peroxide and antibiotic tolerance. J. Bacteriol. **195**:2011–2020.

42. Natori Y, Tagami K, Murakami K, Yoshida S, Tanigawa O, Moh Y, Masuda K, Wada T, Suzuki S, Nanamiya H, Tozawa Y, Kawamura F. 2009. Transcription activity of individual *rrn* operons in *Bacillus subtilis* mutants deficient in (p)ppGpp synthetase genes, *relA*, *yjbM*, and *ywaC*. J. Bacteriol. **191**:4555–4561.

43. Srivatsan A, Han Y, Peng J, Tehranchi AK, Gibbs R, Wang JD, Chen R. 2008. High-precision, whole-genome sequencing of laboratory strains facilitates genetic studies. PLoS Genet. **4**:e1000139. doi:10.1371/journal.pgen.1000139.

44. Mechold U, Potrykus K, Murphy H, Murakami KS, Cashel M. 2013. Differential regulation by ppGpp versus pppGpp in *Escherichia coli*. Nucleic Acids Res. **41**:6175–6189.

45. Choi MY, Wang Y, Wong LL, Lu BT, Chen WY, Huang JD, Tanner JA, Watt RM. 2012. The two PPX-GppA homologues from *Mycobacterium tuberculosis* have distinct biochemical activities. PLoS One **7**:e42561.

46. Somerville CR, Ahmed A. 1979. Mutants of *Escherichia coli* defective in the degradation of guanosine 5′-triphosphate, 3′-diphosphate (pppGpp). Mol. Gen. Genet. **169**:315–323.

47. Keasling JD, Bertsch L, Kornberg A. 1993. Guanosine pentaphosphate phosphohydrolase of *Escherichia coli* is a long-chain exopolyphosphatase. Proc. Natl. Acad. Sci. U. S. A. **90**:7029–7033.

48. Hamel E, Cashel M. 1973. Role of guanine nucleotides in protein synthesis. Elongation factors G and guanosine 5′-triphosphate,3′-diphosphate. Proc. Nat. Acad. Sci, U. S. A. **70**:3250–3254.

49. Suárez CA, Blancato VS, Poncet S, Deutscher J, Magni C. 2011. CcpA represses the expression of the divergent cit operons of *Enterococcus faecalis* through multiple cre sites. BMC Microbiol. **11**:227.

50. Darbon E, Servant P, Poncet S, Deutscher J. 2002. Antitermination by GlpP, catabolite repression via CcpA and inducer exclusion triggered by P-GlpK dephosphorylation control *Bacillus subtilis* glpFK expression. Mol. Microbiol. **43**:1039–1052.

51. Abranches J, Nascimento MM, Zeng L, Browngardt CM, Wen ZT, Rivera MF, Burne RA. 2008. CcpA regulates central metabolism and virulence gene expression in *Streptococcus mutans*. J. Bacteriol. **190**:2340–2349.

52. Deutscher J, Küster E, Bergstedt U, Charrier V, Hillen W. 1995. Protein kinase-dependent HPr/CcpA interaction links glycolytic activity to carbon catabolite repression in gram-positive bacteria. Mol. Microbiol. **15**:1049–1053.

53. Keren I, Wu Y, Inocencio J, Mulcahy LR, Lewis K. 2013. Killing by bactericidal antibiotics does not depend on reactive oxygen species. Science **339**:1213–1216.

54. Liu Y, Imlay JA. 2013. Cell death from antibiotics without the involvement of reactive oxygen species. Science **339**:1210–1213.

55. Kohanski MA, Dwyer DJ, Hayete B, Lawrence CA, Collins JJ. 2007. A common mechanism of cellular death induced by bactericidal antibiotics. Cell **130**:797–810.

56. Cashel M. 1975. Regulation of bacterial ppGpp and pppGpp. Annu. Rev. Microbiol. **29**:301–318.

57. Sonenshein AL. 2007. Control of key metabolic intersections in *Bacillus subtilis*. Nat. Rev. Microbiol. **5**:917–927.

58. Pall ML. 1985. GTP: a central regulator of cellular anabolism. Curr. Top. Cell. Regul. **25**:1–20.

59. Nguyen D, Joshi-Datar A, Lepine F, Bauerle E, Olakanmi O, Beer K, McKay G, Siehnel R, Schafhauser J, Wang Y, Britigan BE, Singh PK. 2011. Active starvation responses mediate antibiotic tolerance in biofilms and nutrient-limited bacteria. Science **334**:982–986.

60. Bokinsky G, Baidoo EE, Akella S, Burd H, Weaver D, Alonso-Gutierrez J, García-Martín H, Lee TS, Keasling JD. 2013. HipA-Triggered growth arrest and beta-lactam tolerance in *Escherichia coli* are mediated by RelA-dependent ppGpp synthesis. J. Bacteriol. **195**:3173–3182.

61. Gao W, Chua K, Davies JK, Newton HJ, Seemann T, Harrison PF, Holmes NE, Rhee HW, Hong JI, Hartland EL, Stinear TP, Howden BP. 2010. Two novel point mutations in clinical *Staphylococcus aureus* reduce linezolid susceptibility and switch on the stringent response to promote persistent infection. PLoS Pathog. **6**:e1000944. doi:10.1371/journal.ppat.1000944.

62. Mwangi MM, Kim C, Chung M, Tsai J, Vijayadamodar G, Benitez M, Jarvie TP, Du L, Tomasz A. 2013. Whole-genome sequencing reveals a link between beta-lactam resistance and synthetases of the alarmone (p)ppGpp in *Staphylococcus aureus*. Microb. Drug Resist. **19**:153–159.

63. Terleckyj B, Willett NP, Shockman GD. 1975. Growth of several cariogenic strains of oral streptococci in a chemically defined medium. Infect. Immun. **11**:649–655.

64. Abranches J, Candella MM, Wen ZT, Baker HV, Burne RA. 2006. Different roles of EIIABMan and EIIGlc in regulation of energy metabolism, biofilm development, and competence in *Streptococcus mutans*. J. Bacteriol. **188**:3748–3756.

65. Zhu A, Romero R, Petty HR. 2010. Amplex UltraRed enhances the sensitivity of fluorimetric pyruvate detection. Anal. Biochem. **403**:123–125.

66. Repizo GD, Mortera P, Magni C. 2011. Disruption of the *alsSD* operon of *Enterococcus faecalis* impairs growth on pyruvate at low pH. Microbiology **157**:2708–2719.

67. Stols L, Gu M, Dieckman L, Raffen R, Collart FR, Donnelly MI. 2002. A new vector for high-throughput, ligation-independent cloning encoding a tobacco etch virus protease cleavage site. Protein Expr. Purif. **25**:8–15.